



## Modelling contact spread of infection in host–parasitoid systems: Vertical transmission of pathogens can cause chaos

Katharine F. Preedy<sup>a</sup>, Pietà G. Schofield<sup>b</sup>, Sijia Liu<sup>c</sup>, Anastasios Matzavinos<sup>c</sup>, Mark A.J. Chaplain<sup>a,\*</sup>, Stephen F. Hubbard<sup>b</sup>

<sup>a</sup> Division of Mathematics, University of Dundee, Dundee DD1 4HN, Scotland, UK

<sup>b</sup> College of Life Sciences, University of Dundee, Dundee DD1 4HN, Scotland, UK

<sup>c</sup> Department of Mathematics, Iowa State University, Ames, IA 50011, USA

### ARTICLE INFO

#### Article history:

Received 18 February 2009

Received in revised form

6 October 2009

Accepted 6 October 2009

Available online 25 October 2009

#### Keywords:

Insect–pathogen interactions

Population dynamics

Infection

Horizontal transmission

Vertical transmission

Vectored diseases

Competition

Chaotic dynamics

### ABSTRACT

All animals and plants are, to some extent, susceptible to disease caused by varying combinations of parasites, viruses and bacteria. In this paper, we develop a mathematical model of contact spread infection to investigate the effect of introducing a parasitoid-vector infection into a one-host–two-parasitoid competition model. We use a system of ordinary differential equations to investigate the separate influences of horizontal and vertical pathogen transmission on a model system appropriate for a variety of competitive situations. Computational simulations and steady-state analysis show that the transient and long-term dynamics exhibited under contact spread infection are highly complex. Horizontal pathogen transmission has a stabilising effect on the system whilst vertical transmission can destabilise it to the point of chaotic fluctuations in population levels. This has implications when considering the introduction of host pathogens for the control of insect vector diseases such as bovine tuberculosis or yellow fever.

© 2009 Elsevier Ltd. All rights reserved.

### 1. Introduction

There is a rapidly accumulating body of evidence demonstrating that many taxa of insects harbour a considerably greater variety of micro-organisms than had previously been suspected, including relatively benign symbionts at one end of a continuum, through to manipulative intracellular parasites at the other (Douglas, 2008; Engelstadter et al., 2007; Kenyon and Hunter, 2007). Microbial pathogens vectored by insects have been mostly well described, as have those infections which kill insects. By contrast, primary endosymbionts have been much less well studied, and secondary endosymbionts remain extremely poorly characterised. As the study of ecological diversity within this last group of bacteria develops it becomes increasingly evident that it is likely that they exercise considerable influence over interspecific interactions, community structure and species biodiversity in insect multi-trophic assemblages (Blaustein and Kiesecker, 2002; Murray, 2002; Collins and Storfer, 2003; Hatcher et al., 2006), and

that they may well play significant roles in the dynamics of both competitive and parasitic relations (Anderson, 1995; Tompkins and Begon, 1999; Bowers and Turner, 1997; Tompkins et al., 2003).

The study of host–pathogen interactions has received a good deal of recent attention (Briggs and Godfray, 1995, 1996; Grenfell and Dobson, 1995; Hudson et al., 2002; Bonsall, 2004; Elderd et al., 2008), but the theoretical investigation of disease dynamics in host–parasitoid systems has not kept pace with associated empirical research (Grenfell and Dobson, 1995; Gulland, 1995; Sait et al., 2000). It has been demonstrated that the inclusion of competitive disease dynamics into a model system can not only promote biodiversity of the system, but also can have sometimes unexpected effects on its dynamics (Holt and Roy, 2007). Preedy et al. (2006), for example, examined the consequences of introducing contact spread host infection into a simple model of a one-host–two-parasitoid system, and found that the presence of the infection not only promoted coexistence of the two parasitoid species, but also that it induced complex population dynamics in the system as a whole, including chaos, and when an explicitly spatial element was introduced into the model, complex spatio-temporal heterogeneity was observed. Clearly, however, infections may be transmitted not only through direct contact between susceptible and infected individuals, but also indirectly through a vector (Bonsall, 2004). In human systems, much has been done on

\* Corresponding author. Tel.: +44 1382 385369; fax: +44 1382 385516.

E-mail addresses: [kath@stams.strath.ac.uk](mailto:kath@stams.strath.ac.uk) (K.F. Preedy), [p.schofield@dundee.ac.uk](mailto:p.schofield@dundee.ac.uk) (P.G. Schofield), [sijialiu@iastate.edu](mailto:sijialiu@iastate.edu) (S. Liu), [tatos@iastate.edu](mailto:tatos@iastate.edu) (A. Matzavinos), [chaplain@maths.dundee.ac.uk](mailto:chaplain@maths.dundee.ac.uk) (M.A. Chaplain), [s.f.hubbard@dundee.ac.uk](mailto:s.f.hubbard@dundee.ac.uk) (S.F. Hubbard).

the spread of malaria and yellow fever via mosquitoes (Aron and May, 1982; Anderson, 1982; Brauer and Castillo-Chavez, 2001), and host–parasitoid models have often been used as metaphors for the dynamics of such infections (see for example Barlow, 2000). However, the primary aim of these models has been to investigate the promulgation of the infection in the host population, and the consequences of the infection for the vectors themselves are often not considered. Indeed, vectored diseases are frequently modelled in host populations by a frequency-dependent process (McCallum et al., 2001) which takes no account of the effect of the pathogen on the vector population and which, when there are two vector (parasitoid) species involved, does not allow for indirect interaction between them.

Thus, a model which explicitly examines the dynamics of parasitoid populations may have very different outcomes from one which considers transmission via parasitoid attack to be a frequency-dependent process. The biology of host infections vectored by parasitoids is highly diverse. In the case of infection of *Drosophila* spp. by the bacterium *Wolbachia*, the vector for transmission of the bacterium may be a parasitoid which is itself infected by *Wolbachia*, from the same or a different strain. Indeed, the parasitoid may act as an agent for inter- as well as intra-species transmission (Haïne et al., 2005). Ascoviruses infecting a host population of lepidoptera can be vectored by parasitoids with whom they may have a mutualistic, commensal or pathogenic relationship (Stasiak et al., 2005). A parasitoid may vector an infection between hosts without being affected itself, as in the case of *Cotesia melanoscelus* which has been shown to vector nuclear polyhedrosis virus (NPV) in the gypsy moth *Lymantria dispar* (Dwyer and Elkinton, 1995; Raimo et al., 1977), and there are various other NPVs recorded from host–parasitoid systems (Nguyen et al., 2005; Briggs et al., 1995). In this paper, we concentrate on the latter case, where the host is susceptible to a nonlethal infection which is carried by the parasitoid. The transmission of disease through parasitoid attack occurs when a parasitoid attacks an infected host, and its ovipositor becomes contaminated and the infection may be passed on when the contaminated ovipositor enters a susceptible host—the “dirty needle effect”. We first describe a model of contact spread infection, then develop it to consider parasitoid vectored infection where only one parasitoid is present, and where there is no vertical transmission of the disease. We then consider a model in which there is perfect vertical transmission, and undertake an analysis of the steady-states of the model and their stability, as well as investigating transient dynamics using computational simulations. Such models are applicable not only to host–parasitoid systems, but also to an understanding of the role of infection in the structure of natural communities. The analytical and computational simulation results in this paper have implications for the effective application of biological control in agro-ecosystems and public health situations, and the general dynamics of disease processes.

## 2. Models and methods

Preedy et al. (2006) developed a mathematical model of the disease dynamics of host–parasitoid systems, modelling the (spatio-temporal) interactions between populations of uninfected hosts, infected hosts and two parasitoid species. They assumed infection was spread between hosts as a contact process, when an infected host encountered a susceptible, uninfected, host. The host population increased via density-dependent logistic growth and was depleted by parasitism by both parasitoid species that was modelled using an Ivlev functional response, an alternative to the

Holling type II response (Sherratt et al., 1995; Pearce et al., 2006; Edelstein-Keshet, 1988; Petrovskii and Malchow, 1999, 2001). Infected hosts and both parasitoid species were subject to a linear death term, and infection was bilinear. It was found that in the absence of infection the weaker parasitoid competitor inevitably went extinct. When infection was included coexistence occurred for a wide parameter range. In the absence of vertical infection either extinction or stability was observed. However, when vertical infection was included, a much richer set of dynamics was observed—depending on the model parameters, the populations tended towards (i) a unique coexistence fixed point (a stable spiral), with the approach to the fixed point being able to be delayed depending on the initial conditions; (ii) a stable limit cycle, or (iii) a chaotic attractor.

In this paper we adapt this approach to a three species system—one host and two parasitoids—where infection is vectored by the parasitoids as a “dirty needle” process, rather than spread as a contact process between infected and susceptible hosts. We assume logistic growth of host populations and parasitoid search is modelled using an Ivlev functional response. However, in this paper we assume that infection is vectored from infected host to uninfected host by parasitoids that have previously parasitised an infected host and have acquired the infection which they carry on their ovipositors. Therefore, we assume the parasitoid may be in one of two infection states—“clean” or “carrier”. We assume that successful parasitism by a carrier parasitoid always infects the host. However, it is possible for a host to be infected but resist parasitism through encapsulation of the parasitoid egg. We assume that there is vertical transmission of infection from infected host to its offspring at some rate that can vary between 0% and 100%. In this paper we present results for the two cases when there is no vertical transmission and when vertical transmission is 100% efficient (intermediate cases of vertical transmission would be straightforward to implement, and given the nature of the results presented in the later sections, we expect these would not introduce any new types of dynamics). We assume a simple linear death rate for parasitoids and an increased death rate of infected hosts over uninfected hosts.

The model therefore consists of six ordinary differential equations, representing the dynamics of  $H_u$  and  $H_i$  the uninfected and infected host populations and  $P_{1u}$ ,  $P_{1i}$ ,  $P_{2u}$ ,  $P_{2i}$ , the noncarrier and carrier populations of the two parasitoid species  $P_1$  and  $P_2$ .

### 2.1. Host dynamics

We assume the host population has logistic density-dependent growth with an intrinsic rate of growth  $\rho_u$  for uninfected hosts and  $\rho_i$  for infected hosts, with a carrying capacity  $H^*$ . We assume vertical transmission is at a rate  $\phi$ , and correspondingly  $(1 - \phi)$  is the fraction of the growth rate of infected hosts that results in susceptible offspring. We model the parasitoid searching efficiency using the Ivlev functional response  $(1 - e^{-\mu H})$ , where  $H = H_u + H_i$  and  $\mu$  is a parameter representing the parasitoid's ability to detect hosts. We assume that parasitoid species  $P_k$  attacks healthy hosts at a maximal rate of  $\alpha_{ku}$  with probability of success  $\beta_{ku}$  and infected hosts at rates  $\alpha_{ki}$  with probability of success  $\beta_{ki}$ . We assume successful parasitism of a host by a carrier parasitoid always leads to infection of the host and that unsuccessful attack of an uninfected host by an infected parasitoid leads to infection of the host at rates of  $\nu_k$ . We also assume the infection induces an additional mortality at a rate  $\xi_i$  in infected hosts. These assumptions lead to the following equations for host

dynamics:

$$\begin{aligned} \frac{dH_u}{dT} &= \underbrace{(\rho_u H_u) \left(1 - \frac{H}{H^*}\right)}_{\text{uninfected host logistic growth}} + \underbrace{(1 - \phi) \rho_i H_i \left(1 - \frac{H}{H^*}\right)}_{\text{recruitment via imperfect transmission}} - \underbrace{\sum_k v_k \alpha_{ku} P_{ku} (1 - e^{-\mu_{ku} H}) \frac{H_u}{H}}_{\text{loss to infection via unsuccessful parasitism by infected species } k} \\ &\quad - \underbrace{\sum_k \beta_{ku} \alpha_{ku} P_{ku} (1 - e^{-\mu_{ku} H}) \frac{H_u}{H}}_{\text{loss to successful parasitism by parasitoid species } k} \\ \frac{dH_i}{dT} &= \underbrace{\phi \rho_i H_i \left(1 - \frac{H}{H^*}\right)}_{\text{infected host logistic growth}} + \underbrace{\sum_k v_k \alpha_{ki} P_{ki} (1 - e^{-\mu_{ki} H}) \frac{H_u}{H}}_{\text{infected host recruitment from failed parasitisms by carriers of species } k} \\ &\quad - \underbrace{\sum_k \beta_{ki} \alpha_{ki} P_{ki} (1 - e^{-\mu_{ki} H}) \frac{H_i}{H}}_{\text{loss to successful parasitism by parasitoid species } k} - \underbrace{\xi_i H_i}_{\text{elevated death rate due to infection}}. \end{aligned} \tag{1}$$

### 2.2. Parasitoid dynamics

We assume that for each species of parasitoid  $P_k$  ( $k = 1, 2$ ) a parasitised uninfected host gives rise to  $\varepsilon_{ku}$  uninfected parasitoids  $P_k$  and each parasitised infected host gives rise to  $\varepsilon_{ki}$  uninfected parasitoids  $P_k$ . It is assumed the infection has no effect on parasitoid mortality, and parasitoids  $P_k$  die at a rate  $\delta_k$ . If the host dies before parasitoid emergence then the juvenile parasitoids fail to mature. We assume that there is no recovery from infection but parasitoids emerging from infected host do not acquire the infection on eclosion. We assume an attack on an infected host by a clean parasitoid  $P_k$  leads to the parasitoid becoming a carrier with probability  $\gamma_k$ . These assumptions lead to the following equations for parasitoid dynamics:

$$\begin{aligned} \frac{dP_{ku}}{dT} &= \underbrace{\varepsilon_{ku} \beta_{ku} \alpha_{ku} P_{ku} (1 - e^{-\mu_{ku} H}) \frac{H_u}{H}}_{\text{recruitment from parasitism by nonviruliferous parasitoids}} + \underbrace{\varepsilon_{ki} \beta_{ki} \alpha_{ki} P_{ki} (1 - e^{-\mu_{ki} H}) \frac{H_i}{H}}_{\text{recruitment from parasitisms by viruliferous parasitoids}} \\ &\quad - \underbrace{\gamma_k \alpha_{ki} P_{ku} (1 - e^{-\mu_{ku} H}) \frac{H_i}{H}}_{\text{loss via acquisition of infection through parasitism of infected hosts}} - \underbrace{\delta_k P_{ku}}_{\text{death}}, \quad k = 1, 2, \\ \frac{dP_{ki}}{dT} &= \underbrace{\gamma_k \alpha_{ki} P_{ku} (1 - e^{-\mu_{ku} H}) \frac{H_i}{H}}_{\text{recruitment via acquisition of infection through parasitism of infected hosts}} - \underbrace{\delta_k P_{ki}}_{\text{death}}, \quad k = 1, 2. \end{aligned} \tag{2}$$

### 2.3. Nondimensionalisation

Combining the host equation (1) with equation (2) for both parasitoid species ( $k = 1, 2$ ) we obtain a system of six ODEs. This system is then nondimensionalised in the usual way using the uninfected host increase rate  $\rho_u$  to scale time, and using the host carrying capacity  $H^*$  to scale population numbers as follows:

$$t = \rho_u T, \quad h_u = \frac{H_u}{H^*}, \quad h_i = \frac{H_i}{H^*}, \quad h = \frac{H}{H^*}, \quad p_{ku} = \frac{P_{ku}}{H^*}, \quad p_{ki} = \frac{P_{ki}}{H^*}.$$

This yields the following nondimensional system of equations:

$$\begin{aligned} \frac{dh_u}{dt} &= (h_u + r(1 - f)h_i)(1 - h) - s_{1u}p_{1u}(1 - e^{-a_{1u}h}) \frac{h_u}{h} \\ &\quad - (s_{1u} + v_1)p_{1i}(1 - e^{-a_{1i}h}) \frac{h_u}{h} - s_{2u}p_{2u}(1 - e^{-a_{2u}h}) \frac{h_u}{h} \\ &\quad - (s_{2u} + v_2)p_{2i}(1 - e^{-a_{2i}h}) \frac{h_u}{h}, \end{aligned}$$

$$\begin{aligned} \frac{dh_i}{dt} &= rfh_i(1 - h) - s_{1i}p_{1u}(1 - e^{-a_{1u}h}) \frac{h_i}{h} \\ &\quad - s_{1i}p_{1i}(1 - e^{-a_{1i}h}) \frac{h_i}{h} + v_1p_{1i}(1 - e^{-a_{1i}h}) \frac{h_u}{h} - s_{2i}p_{2u}(1 - e^{-a_{2u}h}) \frac{h_i}{h} \\ &\quad - s_{2i}p_{2i}(1 - e^{-a_{2i}h}) \frac{h_i}{h} + v_2p_{2i}(1 - e^{-a_{2i}h}) \frac{h_u}{h} - m_i h_i, \end{aligned}$$

$$\begin{aligned} \frac{dp_{1u}}{dt} &= c_{1u}p_{1u}(1 - e^{-a_{1u}h}) \frac{h_u}{h} + c_{1i}p_{1u}(1 - e^{-a_{1u}h}) \frac{h_i}{h} + c_{1v}p_{1i}(1 - e^{-a_{1i}h}) \\ &\quad \times \frac{h_u}{h} + c_{1i}p_{1i}(1 - e^{-a_{1i}h}) \frac{h_i}{h} - g_1p_{1u}(1 - e^{-a_{1u}h}) \frac{h_i}{h} - d_1p_{1u}, \end{aligned}$$

$$\frac{dp_{1i}}{dt} = g_1p_{1u}(1 - e^{-a_{1u}h}) \frac{h_i}{h} - d_1p_{1i},$$

$$\begin{aligned} \frac{dp_{2u}}{dt} &= c_{2u}p_{2u}(1 - e^{-a_{2u}h}) \frac{h_u}{h} + c_{2i}p_{2u}(1 - e^{-a_{2u}h}) \frac{h_i}{h} + c_{2v}p_{2i}(1 - e^{-a_{2i}h}) \\ &\quad \times \frac{h_u}{h} + c_{2i}p_{2i}(1 - e^{-a_{2i}h}) \frac{h_i}{h} - g_2p_{2u}(1 - e^{-a_{2u}h}) \frac{h_i}{h} - d_2p_{2u}, \end{aligned}$$

$$\frac{dp_{2i}}{dt} = g_2p_{2u}(1 - e^{-a_{2u}h}) \frac{h_i}{h} - d_2p_{2i}, \tag{3}$$

where:

- $r = \frac{\rho_i}{\rho_u}$  rate of increase of infected host proportional to uninfected hosts
- $f = \phi$  fidelity of vertical transmission
- $v_k = \frac{v_k \alpha_{ku}}{\rho_u}$  the vector efficiency of parasitoid species  $k = 1, 2$
- $m_i = \frac{\xi_i}{\rho_u}$  the increased host mortality due to infection
- $s_{ku} = \frac{\beta_{ku} \alpha_{ku}}{\rho_u}$  parasitism rate of detected uninfected hosts by parasitoid species  $k = 1, 2$
- $s_{ki} = \frac{\beta_{ki} \alpha_{ki}}{\rho_u}$  parasitism rate of detected infected host by parasitoid species  $k = 1, 2$
- $a_{ku} = \mu_{ku} H^*$  efficiency of detection of uninfected host by parasitoid species  $k = 1, 2$
- $a_{ki} = \mu_{ki} H^*$  efficiency of detection of infected host by parasitoid species  $k = 1, 2$
- $c_{ku} = \frac{\varepsilon_{ku} \beta_{ku} \alpha_{ku}}{\rho_u}$  conversion rate of uninfected host by clean parasitoids of species  $k = 1, 2$
- $c_{ki} = \frac{\varepsilon_{ki} \beta_{ki} \alpha_{ki}}{\rho_u}$  conversion rate of infected hosts by parasitoids of species  $k = 1, 2$
- $c_{kv} = \frac{\varepsilon_{ki} \beta_{ku} \alpha_{ku}}{\rho_u}$  conversion rate of initially uninfected hosts by carrier parasitoids of species  $k = 1, 2$
- $d_k = \frac{\delta_k}{\rho_u}$  death rate of parasitoids of species  $k = 1, 2$
- $g_k = \frac{\gamma_k \alpha_{ki}}{\rho_u}$  infection acquisition rate by parasitoids of species  $k = 1, 2$

The system of equations (3) was solved in Matlab using the ode45 routine (Shampine and Reichelt, 1997) for a range of parameter values discussed below.

## 3. Results

### 3.1. Two species system dynamics

Initially we consider a two species model and we note that setting the initial number of the second parasitoid species

$p_{2u}(0) = P_{0_2} = 0$  gives a two species model. Setting  $f = 0$  gives a model with no-vertical transmission. We use the following set of parameter values:  $s_{1u} = 0.65$ ,  $s_{1i} = 0.45$ , i.e. parasitoids successfully attack infected hosts at a lower rate than uninfected hosts;  $a_{1u} = a_{1i} = 2.5$  i.e. parasitoids detect uninfected and infected hosts at the same efficiency;  $m_i = 0.001$ , i.e. there is a small increase in mortality of hosts due to infection;  $d_1 = 0.2$ ,  $c_{1u} = 0.4$ ,  $c_{1i} = 0.35$  and  $c_{1v} = 0.4$  i.e. parasitoid larvae are less successful in infected hosts than uninfected host, and  $v_1 = 0.5$ ,  $g_1 = 0.5$ .

The system has five biologically realistic fixed points:  $(0, 0, 0, 0)$ ,  $(1, 0, 0, 0)$ ,  $(h_i^*, h_u^*, 0, 0)$ ,  $(h_u^*, 0, p_{1u}^*, 0)$  and  $(h_u^*, h_i^*, p_{1u}^*, p_{1i}^*)$ . There are no fixed points of the form  $(0, h_i^*, p_{1u}^*, 0)$  or  $(0, h_i^*, 0, p_{1i}^*)$  because there is no vertical infection of hosts or parasitoids. All the fixed points are (unstable) saddle points in  $\mathbb{R}^4$  except the coexistence fixed point  $(h_u^*, h_i^*, p_{1u}^*, p_{1i}^*) = (0.246, 0.047, 0.533, 0.112)$ . A standard linear stability analysis confirms that this point is a stable spiral and hence the long-term dynamics of the system tend (asymptotically) to this stable coexistence point.

### 3.2. Three species system dynamics

We now introduce a second parasitoid species  $p_2$  which is a less efficient competitor, but survival of whose larvae in hosts is less affected by the presence of infection. This would mean  $p_2$  has a lower conversion rate than  $p_1$  on uninfected hosts, but this rate is less affected by the infection. This may arise as a result of  $p_1$  laying larger clutches of eggs than  $p_2$ . If this is the case, it is not unreasonable to assume that  $p_1$  is a more efficient vector of the disease than  $p_2$  because it is taking longer to inject more material into the host and therefore giving more opportunity to pass on or acquire infection. Thus, in the examples below we set parameters  $v_1 \geq v_2$  and  $g_1 \geq g_2$ . We also assume that  $p_1$  parasitises healthy hosts at a greater rate than it does infected hosts, whilst  $p_2$  does the reverse.

### 3.3. No vertical transmission

Once again, initially setting  $f = 0$  we have a model where there is no vertical transmission of infection in the host population. We use the parameter set:  $s_{1u} = 0.85$ ,  $s_{2u} = 0.6$ ,  $s_{1i} = 0.7$ ,  $s_{2i} = 0.88$ ,  $a_{ku} = a_{ki} = 2.5$  for both species  $k$ ,  $c_{1u} = 0.9$ ,  $c_{1i} = 0.2$ ,  $c_{1v} = 0.3$ ,  $c_{2u} = 0.4$ ,  $c_{2i} = 0.35$ ,  $c_{2v} = 0.39$ ,  $m_i = 0.005$ ,  $d_1 = 0.19$ ,  $d_2 = 0.11$ ,  $v_1 = 0.63$ ,  $v_2 = 0.51$ ,  $g_1 = 2$ ,  $g_2 = 2$ . In this case, we obtain nine biologically realistic fixed points:  $(0, 0, 0, 0, 0, 0)$ ,  $(1, 0, 0, 0, 0, 0)$ ,  $(h_u^*, h_i^*, 0, 0, 0, 0)$ ,  $(h_u^*, 0, p_{1u}^*, 0, 0, 0)$ ,  $(h_u^*, h_i^*, p_{1u}^*, p_{1i}^*, 0, 0)$ ,  $(h_u^*, 0, 0, 0, p_{2u}^*, 0)$ ,  $(h_u^*, h_i^*, 0, 0, p_{2u}^*, p_{2i}^*)$ ,  $(h_u^*, 0, p_{1u}^*, 0, p_{2u}^*, 0)$  and a coexistence state  $(h_u^*, h_i^*, p_{1u}^*, p_{1i}^*, p_{2u}^*, p_{2i}^*)$ . We note that there is no steady state in which all the parasitoids of a given species are carriers of the infection and if the infection is endemic then, at the steady state, there will be some carriers. All the fixed points are unstable except the coexistence point  $(h_u^*, h_i^*, p_{1u}^*, p_{1i}^*, p_{2u}^*, p_{2i}^*)$  which linear analysis shows to be a stable spiral. From our computational simulations, it is observed that the solution trajectories exhibit initial transient dynamics. These transient dynamics can be extended by changing the initial conditions as shown in Fig. 1 where computational simulations are shown for 5000 time steps. We note that in this case it is not the rise in infected hosts but the increase in the carrier parasitoids,  $p_{1i}$ , which controls the transient high frequency large amplitude oscillations. The  $p_{2u}$  and  $p_{2i}$  population levels take longer to rise.

In order for the coexistence stationary point  $(h_u^*, h_i^*, p_{1u}^*, p_{1i}^*, p_{2u}^*, p_{2i}^*)$  to be stable, it is necessary to have high values of  $g_1$  and  $g_2$ . However, in the original fully dimensional system (1), (2),  $\beta_{ki} + \gamma_k \leq 1$ , so to obtain  $g_1 > 1$  and  $g_2 > 1$  we require that  $\alpha_{ki} > 1$ . In effect, this means that the parasitoid has a high attack rate but a low rate of successful oviposition. If the parasitoid attack rates are lower so that  $v_k < 1$  and  $g_k < 1$  for all  $k = 1, 2$ , we see a situation similar to the case illustrated in Fig. 2 where the same  $s$  and  $a$  values are the same as above and  $c_{1u} = 0.9$ ,  $c_{1i} = 0.2$ ,  $c_{1v} = 0.5$ ,  $c_{2u} = 0.45$ ,  $c_{2i} = 0.3$ ,  $c_{2v} = 0.44$ ,  $m_i = 0.01$ ,  $d_1 = 0.2$ ,  $d_2 = 0.13$ ,  $v_1 = 0.9$ ,  $v_2 = 0.9$ ,  $g_1 = 0.8$ ,  $g_2 = 0.9$ . In this case, the system is

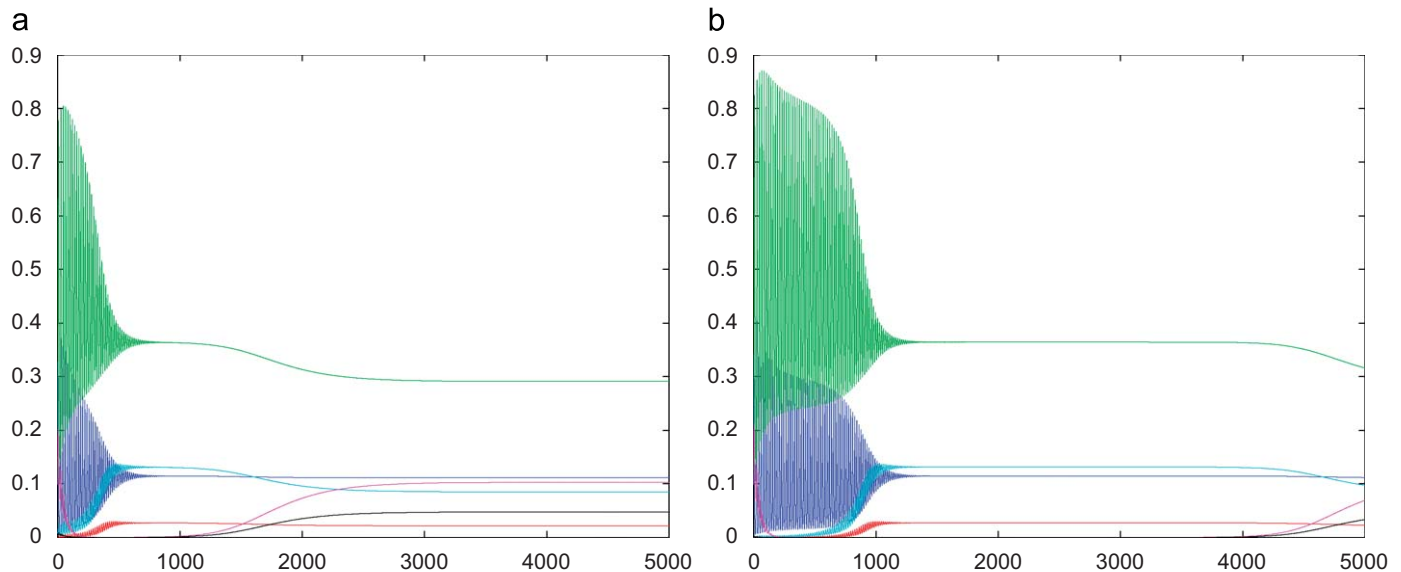


**Fig. 1.** Plots showing the effect of different initial conditions on the system dynamics (up to  $t = 5000$ ) for the model with three species  $h$ ,  $p_1$  and  $p_2$  and no vertical transmission of infection in the host population. The initial transient phase can be extended under different initial conditions. The vertical axis represents relative population density and the horizontal axis time. The different lines represent:  $h_u$  (blue),  $h_i$  (red),  $p_{1u}$  (green),  $p_{1i}$  (cyan),  $p_{2u}$  (magenta) and  $p_{2i}$  (black). Parameter values:  $r = 1$ ,  $f = 0$ ,  $s_{1u} = 0.85$ ,  $s_{2u} = 0.6$ ,  $s_{1i} = 0.7$ ,  $s_{2i} = 0.88$ ,  $a_{ku} = a_{ki} = 2.5$  for all  $k$ ,  $c_{1u} = 0.9$ ,  $c_{1i} = 0.2$ ,  $c_{1v} = 0.3$ ,  $c_{2u} = 0.4$ ,  $c_{2i} = 0.35$ ,  $c_{2v} = 0.39$ ,  $m_i = 0.005$ ,  $d_1 = 0.19$ ,  $d_2 = 0.11$ ,  $v_1 = 0.63$ ,  $v_2 = 0.51$ ,  $g_1 = 2$ ,  $g_2 = 2$ . Initial conditions were (a)  $(0.1, 0.0, 0.1, 0.01, 0.1, 0)$  and (b)  $(0.1, 0.0, 0.1, 0.0, 0.1, 0.001)$ . (For interpretation of the references to colour in this figure legend, the reader is referred to the web version of this article.)

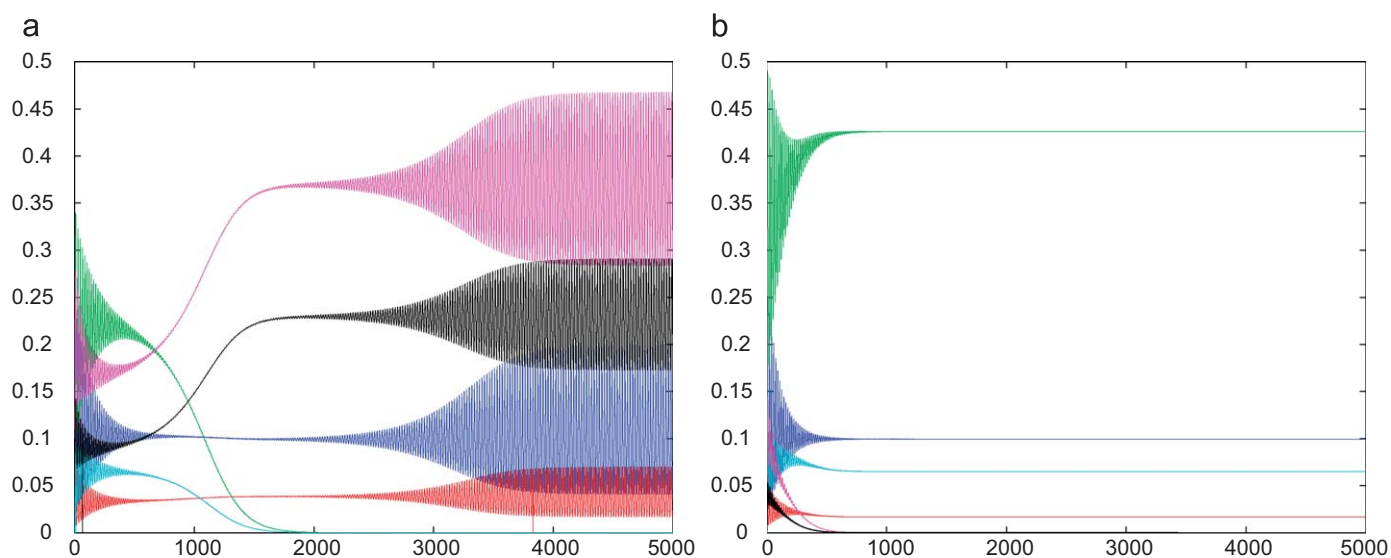


**Fig. 2.** Plots showing the different long-term dynamics (up to  $t = 5000$ ) that occur depending on which parasitoid species goes extinct (bi-stability) for the model with three species  $h$ ,  $p_1$  and  $p_2$  and no vertical transmission of infection in the host population. The vertical axis represents relative population density and the horizontal axis time. The different lines represent:  $h_u$  (blue),  $h_i$  (red),  $p_{1u}$  (green),  $p_{1i}$  (cyan),  $p_{2u}$  (magenta) and  $p_{2i}$  (black). Parameter values  $r = 1$ ,  $f = 0$ ,  $s_{1u} = 0.85$ ,  $s_{2u} = 0.6$ ,  $s_{1i} = 0.7$ ,  $s_{2i} = 0.88$ ,  $a_{ku} = a_{ki} = 2.5$  for all  $k$ ,  $c_{1u} = 0.9$ ,  $c_{1i} = 0.2$ ,  $c_{1v} = 0.5$ ,  $c_{2u} = 0.45$ ,  $c_{2i} = 0.3$ ,  $c_{2v} = 0.44$ ,  $m_i = 0.01$ ,  $d_1 = 0.2$ ,  $d_2 = 0.13$ ,  $v_1 = 0.9$ ,  $v_2 = 0.9$ ,  $g_1 = 0.8$ ,  $g_2 = 0.9$ . Initial conditions were for (a) (0.1, 0.25, 0.001, 0.1, 0.1, 0.01) and (b) (0.1, 0.25, 0.01, 0.001, 0.1, 0.01). (For interpretation of the references to colour in this figure legend, the reader is referred to the web version of this article.)

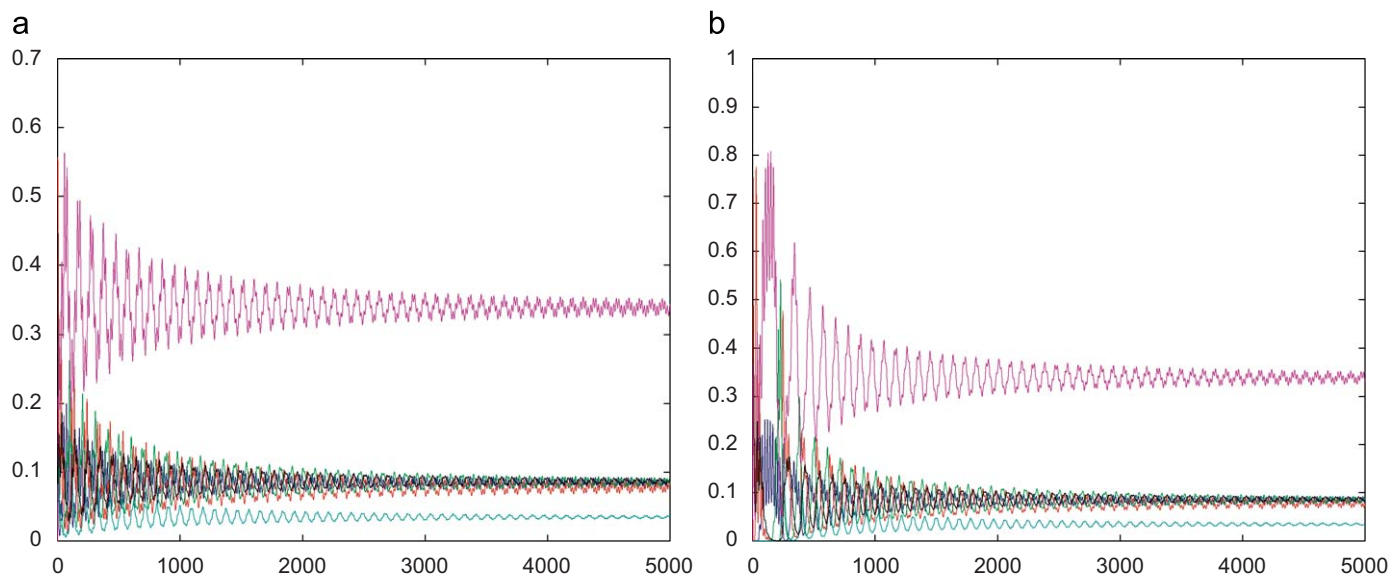


**Fig. 3.** Plots showing the long-term dynamics (up to  $t = 5000$ ) that occur for the model with three species  $h$ ,  $p_1$  and  $p_2$  and perfect vertical transmission of infection in the host population. The population dynamics tend to the stable fixed point of coexistence, with the initial length of the transient period capable of being extended. The vertical axis represents relative population density and the horizontal axis time. The different lines represent:  $h_u$  (blue),  $h_i$  (red),  $p_{1u}$  (green),  $p_{1i}$  (cyan),  $p_{2u}$  (magenta) and  $p_{2i}$  (black). Parameter values  $r = 1$ ,  $f = 1$ ,  $s_{1u} = 0.85$ ,  $s_{2u} = 0.6$ ,  $s_{1i} = 0.7$ ,  $s_{2i} = 0.88$ ,  $a_{ku} = a_{ki} = 2.5$  for all  $k$ ,  $c_{1u} = 0.9$ ,  $c_{1i} = 0.2$ ,  $c_{1v} = 0.3$ ,  $c_{2u} = 0.4$ ,  $c_{2i} = 0.35$ ,  $c_{2v} = 0.39$ ,  $m_i = 0.007$ ,  $d_1 = 0.158$ ,  $d_2 = 0.125$ ,  $v_1 = 0.7$ ,  $v_2 = 0.3$ ,  $g_1 = 0.4$ ,  $g_2 = 0.2$ . Initial conditions were for (a) (0.2, 0.5, 0.1, 0, 0, 0.1) and (b) (0.0001, 0.9, 0, 0.0004, 0, 0.99). (For interpretation of the references to colour in this figure legend, the reader is referred to the web version of this article.)

bi-stable with one or other of the parasitoids going extinct. If  $p_1$  goes extinct then the system is attracted to  $(h_u^*, h_i^*, 0, 0, p_{2u}^*, p_{2i}^*)$  (unstable spiral leading to a stable limit cycle) but if  $p_2$  goes extinct then the system is attracted to  $(h_u^*, h_i^*, p_{1u}^*, p_{1i}^*, 0, 0)$  (stable spiral). The plots shown in Fig. 2 illustrate these two cases.

### 3.4. Perfect vertical transmission

When no vertical infection is included in the model, there are no observed dynamics that might suggest epizootics of infection. However, now setting  $f = 1$  and modelling perfect vertical

transmission from infected hosts to their eggs, we observe very interesting differences in the system behaviour. Using the same searching parameters,  $s_{1u} = 0.85$ ,  $s_{2u} = 0.6$ ,  $s_{1i} = 0.7$ ,  $s_{2i} = 0.88$ ,  $a_{ku} = a_{ki} = 2.5$  for all  $k = 1, 2$ , we examine three particular cases:

Case (i): When  $c_{1u} = 0.9$ ,  $c_{1i} = 0.2$ ,  $c_{1v} = 0.3$ ,  $c_{2u} = 0.4$ ,  $c_{2i} = 0.35$ ,  $c_{2v} = 0.39$ ,  $m_i = 0.007$ ,  $d_1 = 0.158$ ,  $d_2 = 0.125$ ,  $v_1 = 0.7$ ,  $v_2 = 0.3$ ,  $g_1 = 0.4$ ,  $g_2 = 0.2$  we obtain 12 biologically realistic fixed points:

$$(0, 0, 0, 0, 0, 0), (1, 0, 0, 0, 0, 0), (0, h_i^*, 0, 0, 0, 0), (h_u^*, h_i^*, 0, 0, 0, 0), (h_u^*, 0, p_{1u}^*, 0, 0, 0),$$

$$(0, h_i^*, p_{1u}^*, p_{1i}^*, 0, 0), (h_u^*, h_i^*, p_{1u}^*, p_{1i}^*, 0, 0), (h_u^*, 0, 0, 0, p_{2u}^*, 0),$$

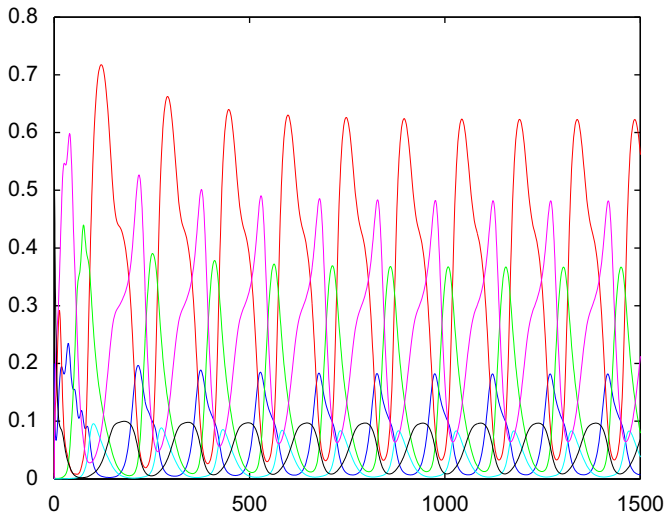


**Fig. 4.** Plots showing the system dynamics (up to  $t = 1500$ ) that occur for the model with three species  $h$ ,  $p_1$  and  $p_2$  and perfect vertical transmission of infection in the host population. In this case, stable limit cycle dynamics are observed. The vertical axis represents relative population density and the horizontal axis time. The lines represent:  $h_u$  (blue),  $h_i$  (red),  $p_{1u}$  (green),  $p_{1i}$  (cyan),  $p_{2u}$  (magenta) and  $p_{2i}$  (black). Parameter values  $r = 1$ ,  $f = 1$ ,  $s_{1u} = 0.85$ ,  $s_{2u} = 0.6$ ,  $s_{1i} = 0.7$ ,  $s_{2i} = 0.88$ ,  $a_{ku} = a_{ki} = 2.5$  for all  $k$ ,  $c_{1u} = 0.9$ ,  $c_{1i} = 0.2$ ,  $c_{1v} = 0.3$ ,  $c_{2u} = 0.45$ ,  $c_{2i} = 0.3$ ,  $c_{2v} = 0.44$ ,  $m_i = 0.005$ ,  $d_1 = 0.2$ ,  $d_2 = 0.2$ ,  $v_1 = 0.63$ ,  $v_2 = 0.51$ ,  $g_1 = 0.1$ ,  $g_2 = 0.1$ . Initial conditions were  $(0.2, 0.005, 0.001, 0, 0, 0.6)$ . (For interpretation of the references to colour in this figure legend, the reader is referred to the web version of this article.)

$$(0, h_i^*, 0, 0, p_{2u}^*, p_{2i}^*), (h_u^*, h_i^*, 0, 0, p_{2u}^*, p_{2i}^*), (h_u^*, 0, p_{1u}^*, 0, p_{2u}^*, 0), (h_u^*, h_i^*, p_{1u}^*, p_{1i}^*, p_{2u}^*, p_{2i}^*).$$

Linear stability analysis shows that  $(h_u^*, h_i^*, p_{1u}^*, p_{1i}^*, p_{2u}^*, p_{2i}^*)$  is a stable spiral in  $\mathbb{R}^6$  but all the other fixed points are unstable. The long-term dynamics of the system therefore tend (asymptotically) to this stable coexistence state and this is illustrated in Fig. 3. A short period of transient dynamics is shown in Fig. 3(b), and by altering the initial conditions it is possible to create extended periods of transient dynamics (not shown). Here, as in Fig. 1, the rise of infection in the host population does not control the transient oscillations, but rather the rise in carrier parasitoids. This is reasonable because the carrier parasitoids are the vectors for horizontal transmission and the results from the previous sections suggest that it is this which affects the transient dynamics.

**Case (ii):** With  $c_{1u} = 0.9$ ,  $c_{1i} = 0.2$ ,  $c_{1v} = 0.3$ ,  $c_{2u} = 0.45$ ,  $c_{2i} = 0.3$ ,  $c_{2v} = 0.44$ ,  $m_i = 0.005$ ,  $d_1 = 0.2$ ,  $d_2 = 0.2$ ,  $v_1 = 0.63$ ,  $v_2 = 0.51$ ,  $g_1 = 0.1$ ,  $g_2 = 0.1$  we see a stable limit cycle as shown in Fig. 4. (The period of the cycle is relatively short so, for clarity, only 1500 time steps are shown.)

These limit cycle dynamics can become quite complex as can be seen from the plots shown in Fig. 5 for the parameter set  $c_{1u} = 0.85$ ,  $c_{1i} = 0.15$ ,  $c_{1v} = 0.3$ ,  $c_{2u} = 0.4$ ,  $c_{2i} = 0.35$ ,  $c_{2v} = 0.39$ ,  $m_i = 0.01$ ,  $d_1 = 0.16$ ,  $d_2 = 0.08$ ,  $v_1 = 0.25$ ,  $v_2 = 0.18$ ,  $g_1 = 0.09$ ,  $g_2 = 0.1$ . Fig. 5a shows the first 15,000 time steps of a typical solution curve, Fig. 5b shows the period from  $t = 45,000$  to 50,000 to illustrate the complex nature of the limit cycle and Fig. 5c shows solution trajectories in a 3d phase-space  $h_u$ ,  $p_{1u}$  and  $p_{2i}$ . Although the system dynamics tending to the limit cycle are complex, the Lyapunov exponent  $\lambda = -0.0051$  is negative when calculated using the MATDS routine from V. Govorukhin, Moscow Univ. (<http://www.math.rsu.ru/mexmat/kvm/matds/>), which does indeed indicate a convergence to the limit cycle and this is visible from Fig. 5c.

**Case (iii):** With  $c_{1u} = 0.9$ ,  $c_{1i} = 0.2$ ,  $c_{1v} = 0.3$ ,  $c_{2u} = 0.46$ ,  $c_{2i} = 0.35$ ,  $c_{2v} = 0.44$ ,  $m_i = 0.007$ ,  $d_1 = 0.158$ ,  $d_2 = 0.1$ ,  $v_1 = 0.7$ ,

$v_2 = 0.3$ ,  $g_1 = 0.4$ ,  $g_2 = 0.2$  the fixed point of coexistence is now an unstable saddle point, and all the other fixed points are also unstable. However, computational simulations show that the solutions remain bounded and tend to what appears to be a chaotic attractor (as is illustrated in Fig. 6c). The normal test for chaotic dynamics is to calculate the largest Lyapunov exponent  $\lambda$  of a system (Gottwald and Melbourne, 2004). If  $\lambda > 0$  then nearby trajectories diverge exponentially whereas if  $\lambda < 0$  then nearby trajectories stay close together. Thus positive  $\lambda$  implies that a system is chaotic and negative  $\lambda$  that it is not. When the Lyapunov exponent is calculated for our system with the current parameter set using the MATDS routine (see above), we find  $\lambda = 0.0012 > 0$  and so demonstrates the existence of chaotic dynamics as can be seen from Fig. 6.

The mathematical analysis and computational simulation results presented in this section show that there is a wide range of dynamic behaviour exhibited by our system (3). The dynamics range from stable coexistence of all three species through oscillatory behaviour caused by the existence of a stable limit cycle, to finally full-blown chaotic dynamics. Thus, from these dynamics we see that, like contact spread infection (cf. Preedy et al., 2006), vectored infection can cause chaotic behaviour in host–parasitoid systems where there is also some degree of vertical infection.

### 3.5. Sensitivity analysis

In this section we undertake a sensitivity analysis of the nondimensionalised system (3) with respect to the full set of (nondimensionalised) parameters. We compute the *normalised* local sensitivity indices and employ the Fourier amplitude sensitivity test (FAST) method for describing the effect of large variations of all parameters on the dependent variables of the system (Varma et al., 1999). In this context, the global sensitivity index of a dependent variable  $x(t)$  with respect to some parameter  $\phi$  is defined as the fraction of the partial variance of  $x(t)$  with respect to  $\phi$  over the total variance of  $x(t)$  with respect to all parameters present in the system. In the following, we use the implementation of the FAST algorithm found in the Systems Biology Toolbox (Schmidt and Jirstrand, 2006).

Fig. 7 shows the results of the FAST analysis as applied to the experimental setting of the two-parasitoid–one-host system with perfect vertical transmission. The figure shows the maximum and minimum global sensitivity indices of the different components of the solution for each nondimensionalised parameter. The larger the size of a bar, the greater the sensitivity of the system to that parameter, and similarly, the smaller the size of a bar, the lesser the sensitivity of the system to that parameter. Interestingly enough the model predicts that, in the context of the two-parasitoid experiment, the parameters with the least influence on the global dynamics are (a) the parameter  $m_i$  representing the increased host mortality due to infection and (b) the conversion rate  $c_{1v}$  of initially uninfected hosts by carrier parasitoids of the first species. Hence,  $m_i$  and  $c_{1v}$  are of little value in controlling the global dynamics of the system.

However, one should be careful not to extrapolate inferences from global sensitivity analysis to local structures in the parameter space. Indeed, the global analysis in Fig. 7 also suggests that variations in the parasitism rate of detected uninfected hosts by parasitoids of the second species affect substantially the global dynamics, and the corresponding parameter  $s_{2u}$  is a potentially good target for controlling the global behaviour of the system. Nonetheless, in the case of the specific instance of the dynamics substantiated by the oscillatory solution shown in Fig. 4, we find that although  $s_{2u}$  is a potentially acceptable target for perturbing

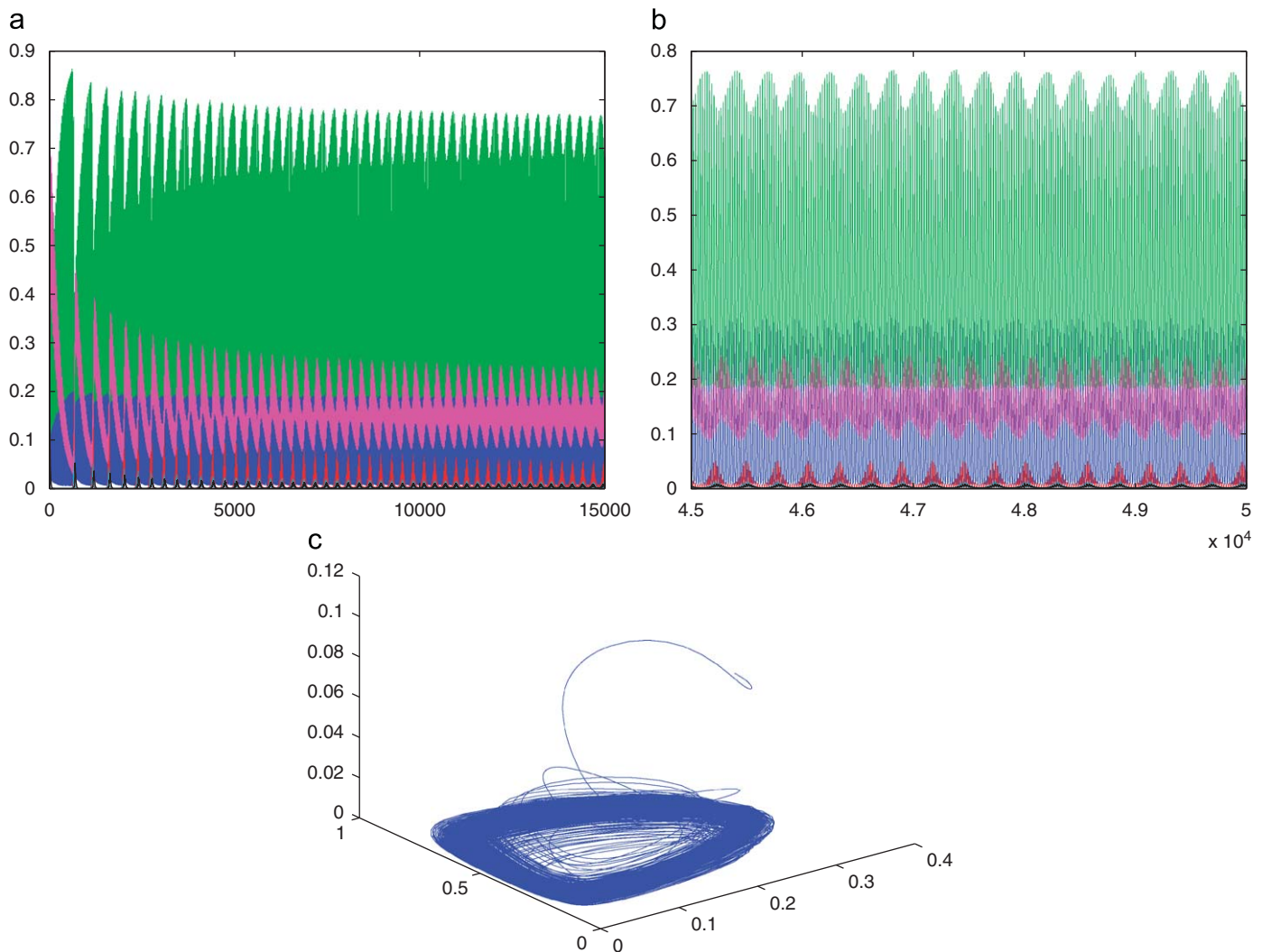


**Fig. 5.** Plots showing the long-term system dynamics that occur for the model with three species  $h$ ,  $p_1$  and  $p_2$  and perfect vertical transmission of infection in the host population. In this case, more complex stable limit cycle dynamics are observed. The vertical axis represents relative population density and the horizontal axis time. The different lines represent:  $h_u$  (blue),  $h_i$  (red),  $p_{1u}$  (green),  $p_{1i}$  (cyan),  $p_{2u}$  (magenta) and  $p_{2i}$  (black). Parameter values  $r = 1$ ,  $f = 1$ ,  $s_{1u} = 0.85$ ,  $s_{2u} = 0.6$ ,  $s_{1i} = 0.7$ ,  $s_{2i} = 0.88$ ,  $a_{ku} = a_{ki} = 2.5$  for all  $k$ ,  $c_{1u} = 0.85$ ,  $c_{1i} = 0.15$ ,  $c_{1v} = 0.3$ ,  $c_{2u} = 0.4$ ,  $c_{2i} = 0.35$ ,  $c_{2v} = 0.39$ ,  $m_i = 0.01$ ,  $d_1 = 0.16$ ,  $d_2 = 0.08$ ,  $v_1 = 0.25$ ,  $v_2 = 0.18$ ,  $g_1 = 0.09$ ,  $g_2 = 0.1$ . (a) Shows the first 15,000 time steps and (b) shows the last 5,000 time steps of a 50,000 time step run. (c) Shows a phase portrait of the solution curve where the axis running from 0 to 1 represents  $h_u$ , the axis running from 0 to 0.4  $p_{1u}$  and the vertical axis  $p_{2i}$ . Initial conditions were (0.2, 0.5, 0.1, 0, 0, 0.1). (For interpretation of the references to colour in this figure legend, the reader is referred to the web version of this article.)

the period of the oscillatory solution, it is a relatively bad choice for controlling the corresponding amplitude. This is shown in Fig. 8 where the normalised local sensitivity indices for the period and amplitude of the oscillatory solution shown in Fig. 4 are plotted. In particular, if  $T(\phi)$  is the period of an oscillatory solution depending on parameter  $\phi$ , then the normalised sensitivity index of  $T(\phi)$  with respect to  $\phi$  is given by

$$S_\phi = \frac{\phi}{T(\phi)} \cdot \frac{dT}{d\phi}(\phi),$$

and a similar definition holds for the normalised sensitivity of the corresponding amplitude (Varma et al., 1999).

As Fig. 7 indicates, the parameter  $a_{2u}$  is associated with the maximum global sensitivity index and has a consistently significant influence on the dynamics of all dependent variables of the system (i.e., the minimum index associated with  $a_{2u}$  is greater than the mean global sensitivity index). Indeed, all populations in the three-species host–parasitoid system are sensitive to perturbations in  $a_{2u}$ , with the latter representing the

efficiency of detection of an uninfected host by the parasitoid species with the lower conversion rate (in our model this is also the parasitoid species the conversion rate of which is less affected by the infection). This observation is consistent with simulation results discussed in this paper, according to which the introduction of a second, less efficient vector of the disease can destabilise the system, whereas the more efficient carrier parasitoid has a stabilising effect. The latter phenomenon is also consistent with the predicted low sensitivity of all populations on parameter  $a_{1u}$ , representing the efficiency of detection of an uninfected host by the parasitoid with the highest conversion rate, as demonstrated in Fig. 7.

In addition to the sensitivity analysis described above, we address the question of whether the  $\omega$ -limit sets identified for system (3) in the presence of vertical transmission correspond to isolated dynamics in the parameter space or whether they persist for a range of parameter values. Direct numerical continuation of the three different types of  $\omega$ -limit sets analysed in this paper (co-existence stable equilibria, limit cycles, chaotic attractors)

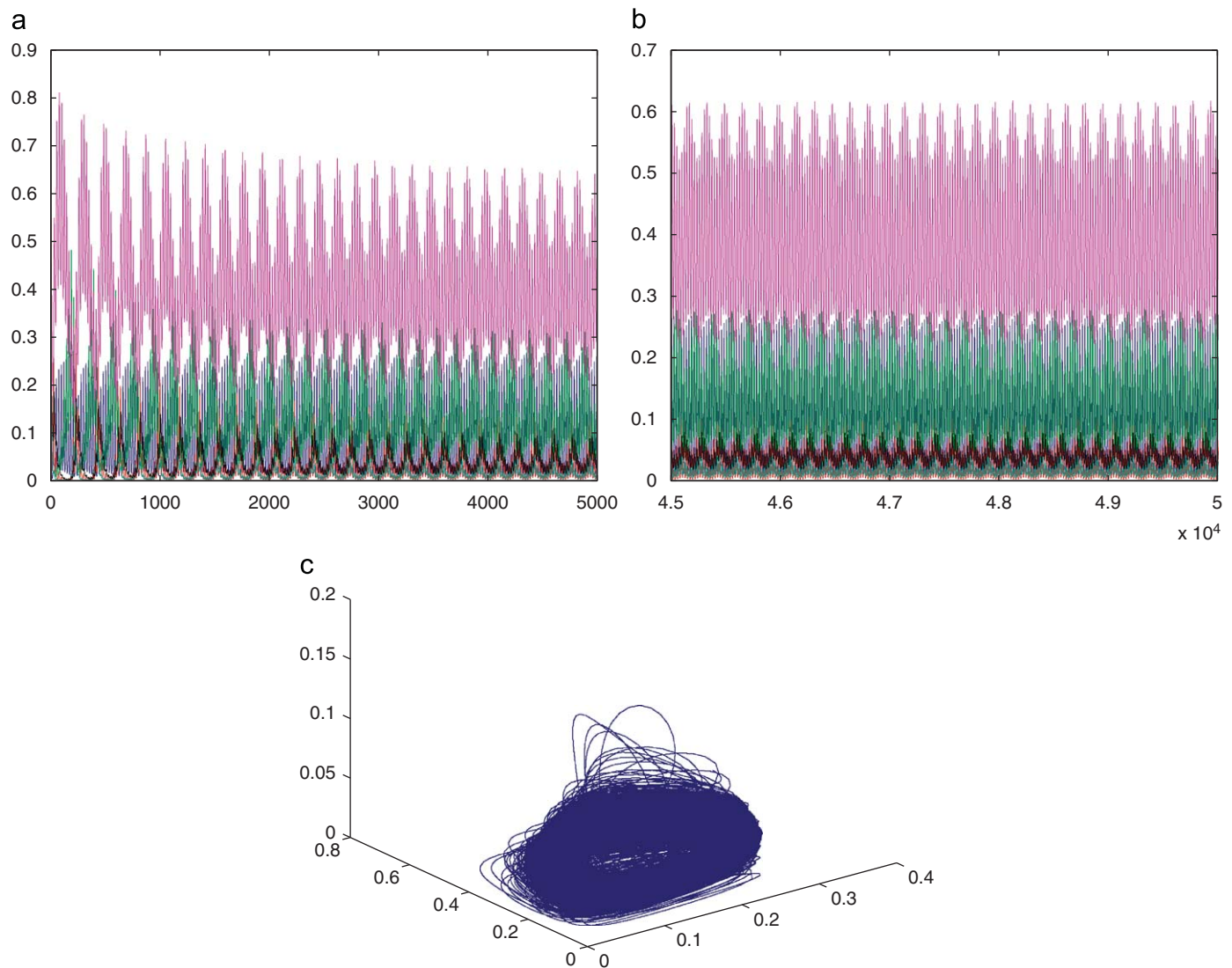


**Fig. 6.** Plots showing the long-term system dynamics that occur for the model with three species  $h$ ,  $p_1$  and  $p_2$  and perfect vertical transmission of infection in the host population. In this case, chaotic dynamics are observed. The vertical axis represents relative population density and the horizontal axis time. The different lines represent:  $h_u$  (blue),  $h_i$  (red),  $p_{1u}$  (green),  $p_{1i}$  (cyan),  $p_{2u}$  (magenta) and  $p_{2i}$  (black). Parameter values  $r = 1$ ,  $f = 1$ ,  $s_{1u} = 0.85$ ,  $s_{2u} = 0.6$ ,  $s_{1i} = 0.7$ ,  $s_{2i} = 0.88$ ,  $a_{ku} = a_{ki} = 2.5$  for all  $k$ ,  $c_{1u} = 0.9$ ,  $c_{1i} = 0.2$ ,  $c_{1v} = 0.3$ ,  $c_{2u} = 0.46$ ,  $c_{2i} = 0.35$ ,  $c_{2v} = 0.44$ ,  $m_i = 0.007$ ,  $d_1 = 0.158$ ,  $d_2 = 0.1$ ,  $v_1 = 0.7$ ,  $v_2 = 0.3$ ,  $g_1 = 0.4$ ,  $g_2 = 0.2$ . (a) shows the first 5000 time steps and (b) shows the last 5000 time steps of a 50,000 time step run. (c) Chaotic attractor in the 3d phase space of  $h_u$ ,  $p_{1u}$  and  $p_{2i}$ . Initial conditions were (0.2, 0.5, 0.1, 0, 0, 0.1). (For interpretation of the references to colour in this figure legend, the reader is referred to the web version of this article.)

shows that all three types persist for wide ranges of parameter values. Fig. 9 shows the limit cycle and strange attractor dynamics associated with system (3) for two distinct sets of parameter values. The plot shows the projection of the corresponding dynamics to the  $h_u - h_i - p_{1u}$  space. Fig. 10 shows specific instances of the numerical continuation of these dynamics with respect to parameters  $s_{1u}$  and  $c_{2i}$ . The figure readily demonstrates that, by smoothly varying these parameters, the strange attractor of Fig. 9 is gradually transformed to a limit cycle, and an extensive numerical continuation analysis has confirmed that both  $\omega$ -limit sets persist for wide ranges of parameter values.

#### 4. Discussion

This paper develops a mathematical model of contact transmitted host infection to consider the effect of introducing parasitoid-vectored host infection to a one-host-two-parasitoid

competition model. Although the model is more complex than a contact transmission model, this additional complexity is necessary to track the population of carrier parasitoids which allows us to separate the influences of horizontal and vertical transmission, and helps to clarify the relative importance of the two transmission routes. The results show that both the complex transient and long-term dynamics induced by contact transmitted infection are highly complex. It is possible for the vector transmitted infection to become endemic with only a single parasitoid vector, but if this happens the fixed point of coexistence is always a stable attractor (spiral). The introduction of a second parasitoid to the system induces an initial transient phase of high amplitude, high frequency oscillations, the period of which depends on the initial conditions of the system. This suggests that the introduction of a second parasitoid can destabilise the system, a conclusion relevant to the introduction of nonnative species for bio-control initiatives. These transient dynamics are not stabilised by the rise in the infected host population, but rather by the increase in the

population of the more efficient carrier parasitoid. This remains the case when vertical transmission is included in the model, suggesting that horizontal infection is what stabilises the transient oscillations. Where there is no vertical transmission of the infection, the system either has a fixed point of coexistence which is a stable spiral, or we observe a bi-stability where one or other of the parasitoid species goes extinct. When vertical infection is introduced to the system, the dynamics become more complex with the appearance of a stable limit cycle and eventually may become chaotic.

Of course, these dynamics were observed using a selected set (or few sets) of parameter values. Therefore, in order to investigate

how widespread or typical this behaviour is for the model, we undertook several parameter sensitivity analyses of the system. Firstly, using the FAST algorithm (Varma et al., 1999; Schmidt and Jirstrand, 2006) we showed the influence of each parameter on the global dynamics of the system. Additionally, using the normalised sensitivity index (Varma et al., 1999) we studied the effect of variations in each parameter on the local structures of the system i.e. the period and amplitude of the limit cycle. Finally, an extensive direct numerical continuation revealed that all three types of  $\omega$ - limit set observed in the system (co-existence stable

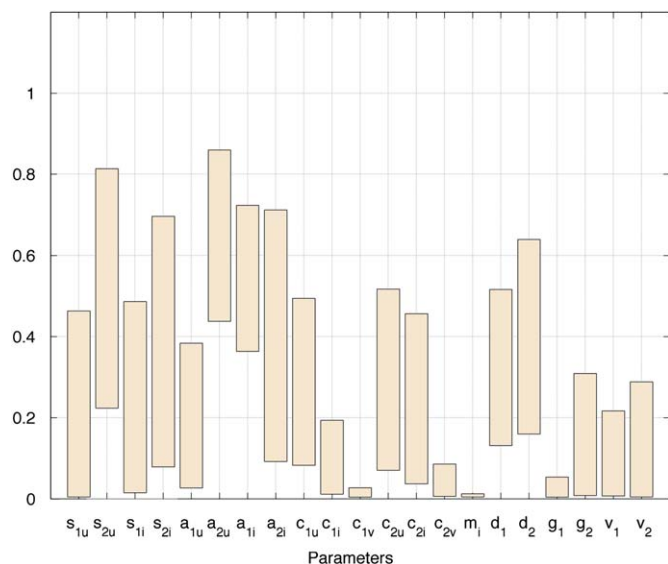


**Fig. 7.** Global sensitivity analysis of the nondimensionalised system (3) in the case of the two-parasitoid–one-host system with perfect vertical transmission. Every bar in the diagram shows the maximum and minimum global sensitivity indices of the different components of the solution for each nondimensionalised parameter.

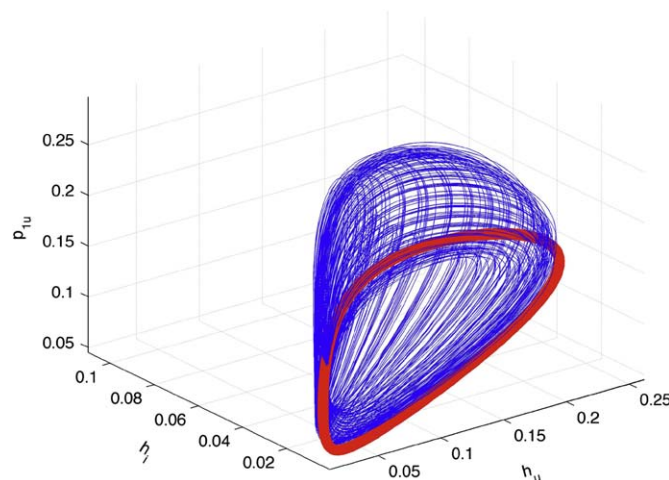
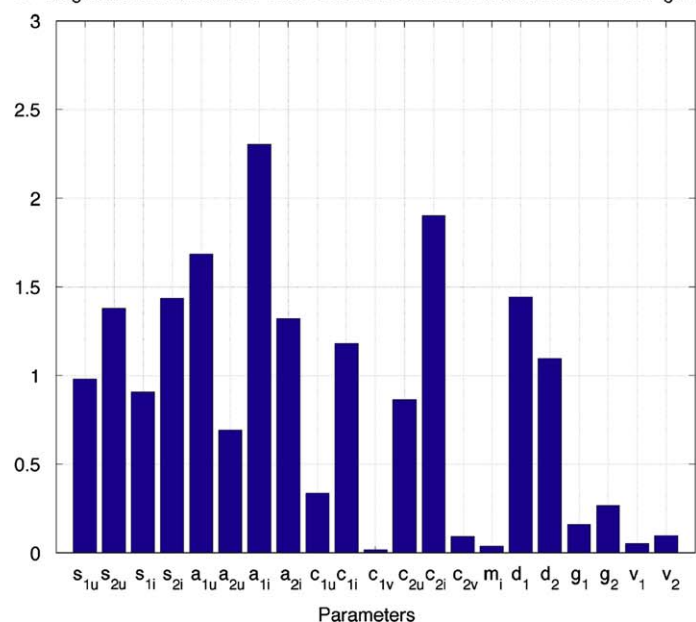


**Fig. 9.** Limit cycle (red) and strange attractor (blue) dynamics associated with system (3) for different parameter values. The plot shows the projection of the corresponding dynamics to the  $h_u - h_i - p_{1u}$  space. By smoothly varying specific parameters of the system one can transform the limit cycle to the strange attractor. Both  $\omega$ - limit sets persist for a range of parameter values and are not isolated structures in the parameter space. The strange attractor shown here corresponds to the parameter values of Fig. 6 but  $c_{1u} = 0.85$ . The limit cycle corresponds to the parameter values used for the strange attractor but  $s_{1u} = 1.05$  and  $c_{2i} = 0.55$ . (For interpretation of the references to colour in this figure legend, the reader is referred to the web version of this article.)

**a** Magnitude of Normalized Period Sensitivities for the Simulation Shown on Fig. 4



**b** Normalized Amplitude Sensitivities (Min-Max) for the Simulation Shown on Fig. 4

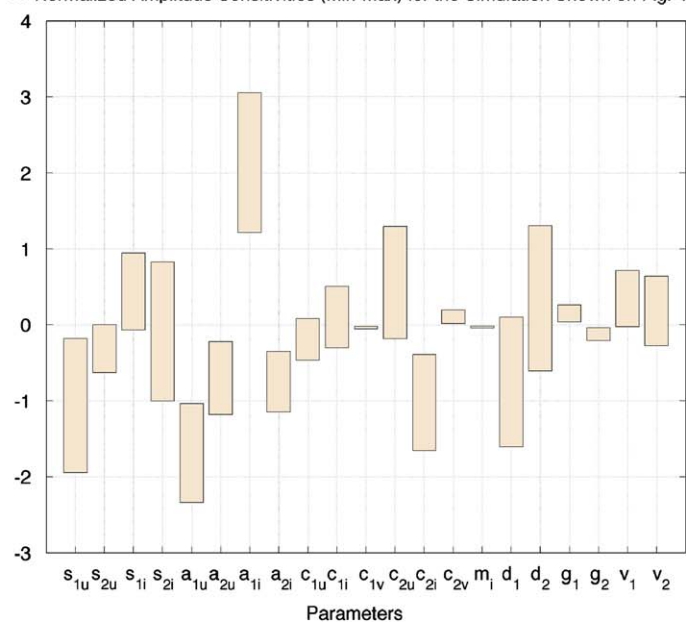


**Fig. 8.** Local sensitivity analysis of (a) the period and (b) the amplitude of the oscillatory solution shown in Fig. 4. See text for the definition of the normalised local sensitivity index.

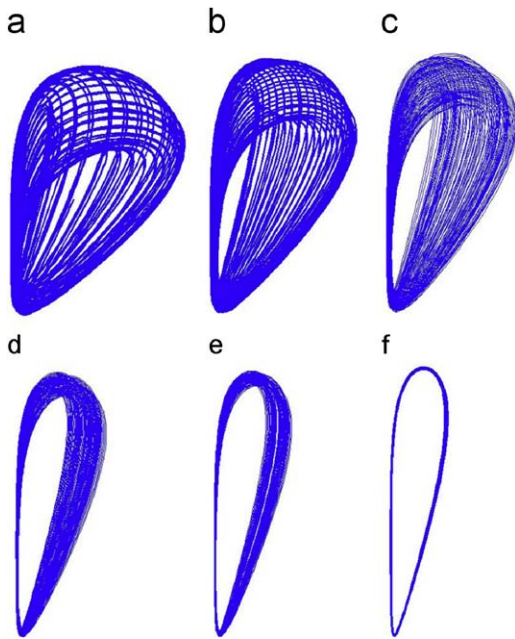


**Fig. 10.** Sequence of  $\omega$ -limit sets of system (3) for different parameter values. The attractor dynamics shown in (a) correspond to the strange attractor of Fig. 9. By smoothly varying parameters  $s_{1u}$  and  $c_{2i}$  the strange attractor is transformed to a limit cycle. As discussed in the text with reference to Fig. 9, both types of  $\omega$ -limit sets persist for a range of parameter values and are not isolated structures in the parameter space. (a)  $s_{1u} = 0.85$ ,  $c_{2i} = 0.35$ . (b)  $s_{1u} = 0.855$ ,  $c_{2i} = 0.355$ . (c)  $s_{1u} = 0.86$ ,  $c_{2i} = 0.36$ . (d)  $s_{1u} = 0.87$ ,  $c_{2i} = 0.37$ . (e)  $s_{1u} = 0.88$ ,  $c_{2i} = 0.38$ . (f)  $s_{1u} = 0.89$ ,  $c_{2i} = 0.39$ .

equilibria, limit cycles, chaotic attractors) exist and persist for wide ranges of parameter values.

It is known that predator–prey systems may exhibit chaotic behaviour under certain initial conditions when a spatial element is considered (Petrovskii and Malchow, 2001). However, in these models, irregular spatio-temporal behaviour only occurs under suitably perturbed initial conditions. Highly heterogeneous spatio-temporal dynamics have also been observed in predator–prey systems with limit cycle kinetics (Sherratt et al., 1995). The model considered here exhibits chaotic behaviour induced by biologically realistic mechanisms and under the assumption of spatial homogeneity. Although we have not considered a spatial model here (e.g. with the diffusion of all species), it is possible to anticipate (qualitatively) the spatio-temporal dynamics of such a spatial model from the three basic underlying types of behaviour shown in the long-term (asymptotic) behaviour of the trajectories of the system i.e. the system tends to either a single coexistence fixed point, or a stable limit cycle or a chaotic attractor. These underlying temporal dynamics imply that a corresponding spatial model would exhibit progressively more complex “waves of invasion”, mirroring the results of Preedy et al. (2006). The spatio-temporal dynamics of such a system add an extra layer of complexity to the already complex underlying temporal population dynamics and have implications for the spatial-spread and treatment of disease.

Therefore, it is possible that the chaotic behaviour shown by the model may be an intrinsic property of the trophic association which it mimics. The stabilising effects of infection seem mainly to act horizontally within a generation, whilst the destabilising effects seem primarily to operate vertically. This would suggest that in considering the introduction of infection for the purposes of bio-control, it may be more appropriate to consider those which have no vertical transmission. In this respect, the infection would act as a “live” insecticide, with the parasitoids as the

disseminators of the infection. Even if there were no synergy between parasitism and host infection, which is probably unlikely, the overall effect on the host death rate would be to increase it within a single generation. If control were seen as inoculative, then this would increase the impact of a parasitoid species on a target pest population. Similarly, in situations where an endemic infection has an element of vertical transmission, the consequences of the invasion of a second competing parasitoid may dramatically destabilise the system. This should caution against the automatic assumption, often made, that multiple natural enemies will always be more effective in controlling a pest species than a single parasitoid species. Transient high amplitude high frequency oscillations were seen with the introduction of a second parasitoid vector and these were controlled by the rise in population of the more efficient vector. We have discussed host–parasitoid interactions in general above, but such systems form a good metaphor for predator–prey and host–pathogen interactions. There are many diseases, such as louping-ill virus (LIV), bovine tuberculosis, malaria and yellow fever which are transmitted via a vector, and which may have more than one species or form of vector. The findings of this paper have implications for the strategies used in control of such infections.

### Acknowledgements

The work of K.P. was supported by a BBSRC PhD studentship. M.A.J.C. acknowledges the support of a Leverhulme Trust Personal Research Fellowship.

### References

- Anderson, R.M., 1995. Evolutionary pressures in the spread and persistence of infectious agents in vertebrate populations. *Parasitology* 111, S15–S31.
- Anderson, R.M. (Ed.), 1982. *Population Dynamics of Infectious Diseases: Theory and Applications*. Chapman and Hall, London, New York.
- Aron, J.L., May, R.M., 1982. Population dynamics of malaria. In: Anderson, R.M. (Ed.), *Population Dynamics of Infectious Diseases: Theory and Applications*. Chapman and Hall, London, New York.
- Barlow, N.D., 2000. Non-linear transmission and simple models for bovine tuberculosis. *Journal of Animal Ecology* 69 (4), 703–713.
- Blaustein, A.R., Kiesecker, J.M., 2002. Complexity in conservation: lessons from the global decline of amphibian populations. *Ecology Letters* 5, 597–608.
- Bonsall, M.B., 2004. The impact of diseases and pathogens on insect population dynamics. *Physiological Entomology* 29, 223–236.
- Bowers, R.G., Turner, J., 1997. Community structure and the interplay between interspecific infection and competition. *Journal of Theoretical Biology* 187, 95–109.
- Brauer, F., Castillo-Chavez, C., 2001. *Mathematical Models in Population Biology and Epidemiology*. Springer, New York.
- Briggs, C.J., Godfray, H.C.J., 1995. The dynamics of insect–pathogen interactions in stage-structured populations. *American Naturalist* 145, 855–887.
- Briggs, C.J., Godfray, H.C.J., 1996. The dynamics of insect–pathogen interactions in seasonal environments. *Theoretical Population Biology* 50, 149–177.
- Briggs, C.J., Hails, R.S., Barlow, N.D., Godfray, H.C.J., 1995. The dynamics of insect–pathogen interactions. In: Grenfell, B.T., Dobson, A.P. (Eds.), *Ecology of Infectious Diseases in Natural Populations*. Cambridge University Press, Cambridge, pp. 295–326.
- Collins, J.P., Storfer, A., 2003. Global amphibian declines: sorting the hypotheses. *Diversity and Distributions* 9, 89–98.
- Douglas, A.E., 2008. Conflict, cheats and the persistence of symbioses. *New Phytologist* 177, 849–858.
- Dwyer, G., Elkinton, J.S., 1995. Host dispersal and the spatial spread of insect pathogens. *Ecology* 76 (4), 1262–1275.
- Edelstein-Keshet, L., 1988. *Mathematical Models in Biology*. Birkhäuser Mathematics Series. McGraw-Hill, New York.
- Elder, B.D., Dushoff, J., Dwyer, G., 2008. Host pathogen interaction, insect outbreaks, and natural selection for disease resistance. *American Naturalist* 20, 685–695.
- Engelstadter, J., Hammerstein, P., Hurst, G.G.D., 2007. The evolution of endosymbiont density in doubly infected host species. *Journal of Evolutionary Biology* 172 (6), 829–842.
- Gottwald, G.A., Melbourne, I., 2004. A new test for chaos in deterministic systems. *Proceedings of the Royal Society* 460, 603–611.
- Grenfell, B.T., Dobson, A.P. (Eds.), 1995. *Ecology of Infectious Diseases in Natural Populations*. Cambridge University Press, Cambridge.
- Gulland, F.M.D., 1995. The impact of infectious diseases in wild animal populations—a review. In: Grenfell, B.T., Dobson, A.P. (Eds.), *Ecology of*

- Infectious Diseases in Natural Populations. Cambridge University Press, Cambridge, pp. 20–51.
- Haine, E.R., Pickup, N.J., Cook, J.M., 2005. Horizontal transmission of *Wolbachia* in *Drosophila* community. *Ecological Entomology* 30, 464–472.
- Hatcher, M.J., Dick, J.T.A., Dunn, A.M., 2006. How parasites affect interactions between competitors and predators. *Ecology Letters* 9, 1253–1271.
- Holt, R.D., Roy, M., 2007. Predation can increase the prevalence of infectious disease. *American Naturalist* 169 (5), 690–699.
- Hudson, P.J., Rizzoli, A., Grenfell, B.T., Heesterbeek, H., Dobson, A.P. (Eds.), 2002. *The Ecology of Wildlife Diseases*. Oxford University Press, Oxford.
- Kenyon, S.G., Hunter, M.S., 2007. Manipulation of oviposition choice of the parasitoid wasp *Encarsia pergandiella* by the endosymbiotic bacterium *Cardinium*. *Journal of Evolutionary Biology* 20, 707–716.
- McCallum, H., Barlow, N., Hone, J., 2001. How should pathogen transmission be modelled?. *Trends in Ecology and Evolution* 16, 295–300.
- Murray, J.D., 2002. *Mathematical Biology. I: An Introduction*, third ed Springer, Berlin.
- Nguyen, D.H., Nakai, M., Takatsuka, J., Okuno, S., Ishii, T., Kunimi, Y., 2005. Interaction between a nucleopolyhedrovirus and the braconid parasitoid *Meteorus pulchricornis* (hymenoptera: Braconidae) in the larvae of *Spodoptera litura* (lepidoptera: Noctuidae). *Applied Entomology and Zoology* 40 (2), 325–334.
- Pearce, I.G., Chaplain, M.A.J., Schofield, P.G., Anderson, A.R.A., Hubbard, S.F., 2006. Modelling the spatio-temporal dynamics of multi-species host-parasitoid interactions: heterogeneous patterns and ecological implications. *Journal of Theoretical Biology* 241 (4), 876–886.
- Petrovskii, S.V., Malchow, H., 1999. A minimal model of pattern formation in a predator–prey system. *Mathematical and Computer Modelling* 29, 49–63.
- Petrovskii, S.V., Malchow, H., 2001. Wave of chaos: new mechanism of pattern formation in spatio-temporal population dynamics. *Theoretical Population Biology* 59, 157–174.
- Preedy, K.F., Schofield, P.G., Chaplain, M.A.J., Hubbard, S.F., 2006. Disease induced dynamics in host–parasitoid systems: chaos and coexistence. *Journal of the Royal Society Interface* 4, 463–471.
- Raimo, B., Reardon, R.C., Podgwaite, J.D., 1977. Vectoring of gypsy moth nuclear polyhedrosis virus by *Apanteles melanoceus* (hym: Braconidae). *Entomophaga* 22, 207–215.
- Sait, S.M., Liu, W.C., Thompson, D.J., Godfray, H.C.J., Begon, M., 2000. Invasion sequence affects predator–prey dynamics in a multi-species interaction. *Nature* 405, 448–450.
- Schmidt, H., Jirstrand, M., 2006. Systems biology toolbox for MATLAB: a computational platform for research in systems biology. *Bioinformatics* 22, 514–515.
- Sherratt, J.A., Lewis, M.A., Fowler, A., 1995. Ecological chaos in the wake of invasion. *Proceedings of the National Academy Science* 92, 2524–2528.
- Shampine, L.F., Reichelt, M.W., 1997. The MATLAB ODE suite. *SIAM Journal on Scientific Computing* 18, 1–22.
- Stasiak, K., Renault, S., Fedrici, B.A., Bigot, Y., 2005. Characteristics of pathogenic and mutualistic relationships of ascoviruses in field populations of parasitoid wasps. *Journal of Insect Physiology* 51, 103–115.
- Tompkins, D.M., Begon, M., 1999. Parasites can regulate wildlife populations. *Parasitology Today* 15, 311–313.
- Tompkins, D.M., White, A.R., Boots, M., 2003. Ecological replacement of native red squirrels by invasive greys driven by disease. *Ecology Letters* 6, 189–196.
- Varma, A., Morbidelli, M., Wu, H., 1999. *Parametric Sensitivity in Chemical Systems*. Cambridge University Press, Cambridge.